Synthesis of a rhodamine antimony analog

George Rajendra Kumar, Mengxi Yang, Benyu Zhou, and François P. Gabbaï*

Department of Chemistry, Texas A&M University, College Station, USA, francois@tamu.edu

Abstract: We describe the synthesis, structure and characterization of an antimony-rhodamine derivative, with a phenyl-antimony moiety installed at the 10'-position of the central ring. This compound is a red fluorophore (λ_{em} = 655 nm) with a quantum yield of 12% in acetonitrile.

TOC graphic

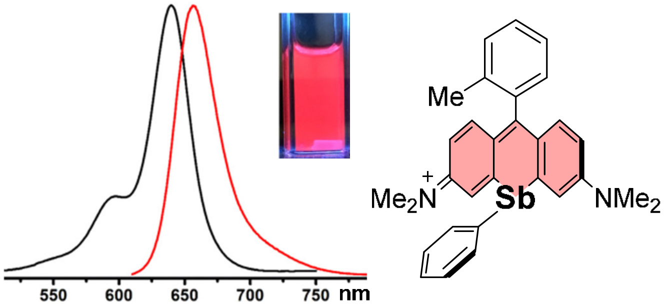

Keywords: organoantimony compounds, rhodamine, fluorescence, synthesis, structure

The incorporation of antimony in emissive derivatives is drawing a great deal of attention in our research because of application in anion sensing.[1-4] Examples of such compounds include organoantimony derivatives functionalized by fluorescent units such as anthrancene,[5] pyrene,[6] perylene[6] and BODIPY,[7] among others. In all cases, the antimony moiety stands at the periphery of the fluorophore. Efforts to integrate the antimony atom within the chromophore structure, as in the case of **1**,[8, 9] **2**,[10] and **3**[11] are much scarcer (Figure 1). These compounds are appealing because of the intimate connection that exists between the antimony atom and the p-conjugated chromophore. Absent from the literature are efforts describing the inclusion of antimony into prominent organic fluorophores such as rhodamine. This situation is somewhat surprising especially if one considers that many other main group moieties have been successfully incorporated at the rhodamine 10'-position occupied by an oxygen atom in the parent compound.[12-16] Looking at the lower part of the p-block, it is also worth noting that main group rhodamines based on tin,[17] tellurium,[18, 19] and bismuth ([**4**]$^+$, Figure 1)[20] are known, making the absence of the antimony analog even more noticeable. As part of our ongoing program in the chemistry of antimony-based fluorescent materials, we now describe the synthesis, structure and properties of an antimony-rhodamine, also referred to as a stibarhodamine.

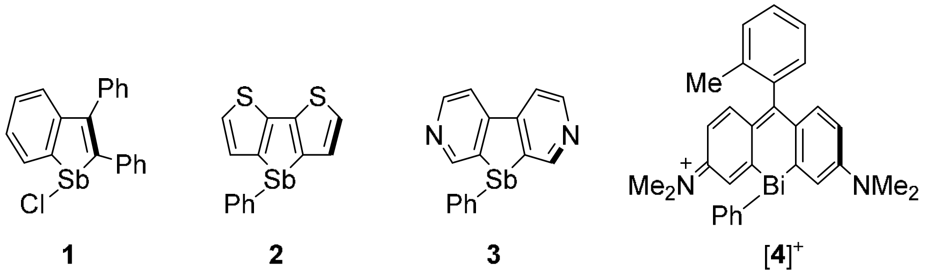

Figure 1: Examples of derivatives (**1**-**3**) featuring an antimony atom incorporated in a π-conjugated chromophore, and the known bismuth rhodamine analog [**4**]$^+$.

Based on literature precedents,[21] the starting dibromide **5** was lithiated in THF at low temperature (-78 °C) and allowed to react with $PhSbCl_2$. After warming up the reaction mixture and allowing it to reflux for several hours, all volatile components were removed and the residue subjected to oxidation with p-chloranil in the presence of trifluoroacetic acid (TFAH). The resulting stibarhodamine ([**6**][TFA]) was purified by chromatography and obtained in a 5 % yield. The ^{1}H NMR spectrum of [**6**][TFA] displays the expected resonance including on at 3.37 ppm corresponding to dimethylamino group. The trifluoroacetate anion ($[TFA]^-$) was exchange with $[PF_6]^-$ using a large excess of KPF_6 which was added to a methanol (10 mL) solution of [**6**][TFA]. Crude [**6**][PF_6] was isolated by evaporation of the mixture and washing with water. Single crystals suitable of [**6**][PF_6] were obtained from slow diffusion of diethyl ether into a dichloromethane solution of the salt.† Salt [**6**][PF_6] crystalizes in the triclinic *P*-1 space group with two molecules of $[\mathbf{6}]^+$ and two $[PF_6]^-$ anions in the asymmetric unit. The two independent molecules of $[\mathbf{6}]^+$ display very similar structure (Figure 2). The central ring of the rhodamine unit is very slightly puckered with the antimony atom siting 0.24 or 0.25 Å above the plane defined by the carbon atoms at the 9', 4a', 8a', 9a' and 10a' position. With all C-Sb-C angles approaching the value of 90°, the antimony-bound phenyl group is arranged in a perpendicular fashion with respect to the planar stibarhodamine chromophore. Such an orientation is reminiscent of that observed in the case of **2**,[10] and **3**[11]. The two *N,N*-dimethylamino groups adopts a trigonal planar geometry about nitrogen, indicating the expected conjugation of the nitrogen lone pair with the rest of the chromophore (Figure 1).

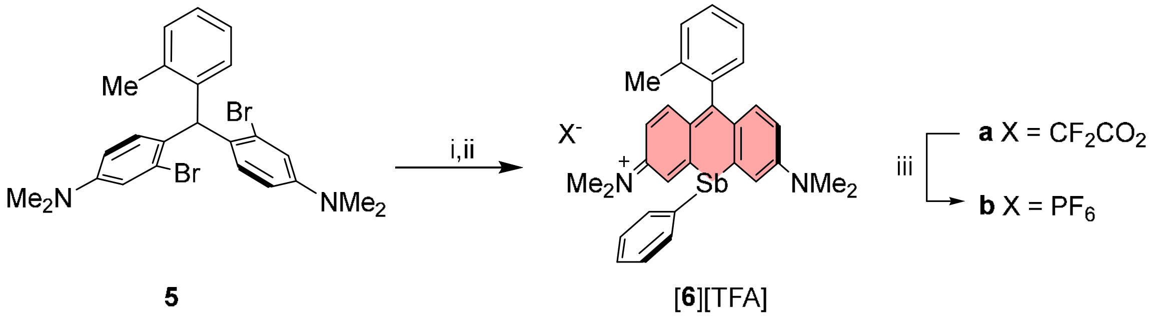

Scheme 1: **Scheme 1** *Reagents and conditions:* i, BuLi (2 equiv.), THF, -78 °C, then $PhSbCl_2$, reflux; ii, *p*-chloranil, CH_2Cl_2, 0°C, 1 hour, then column chromatography, Al_2O_3, 0.1% CF_3CO_2H in $MeOH/CH_2Cl_2$ 95/5 (v/v); iii, KPF_6, MeOH, 25°C, 2 hours.

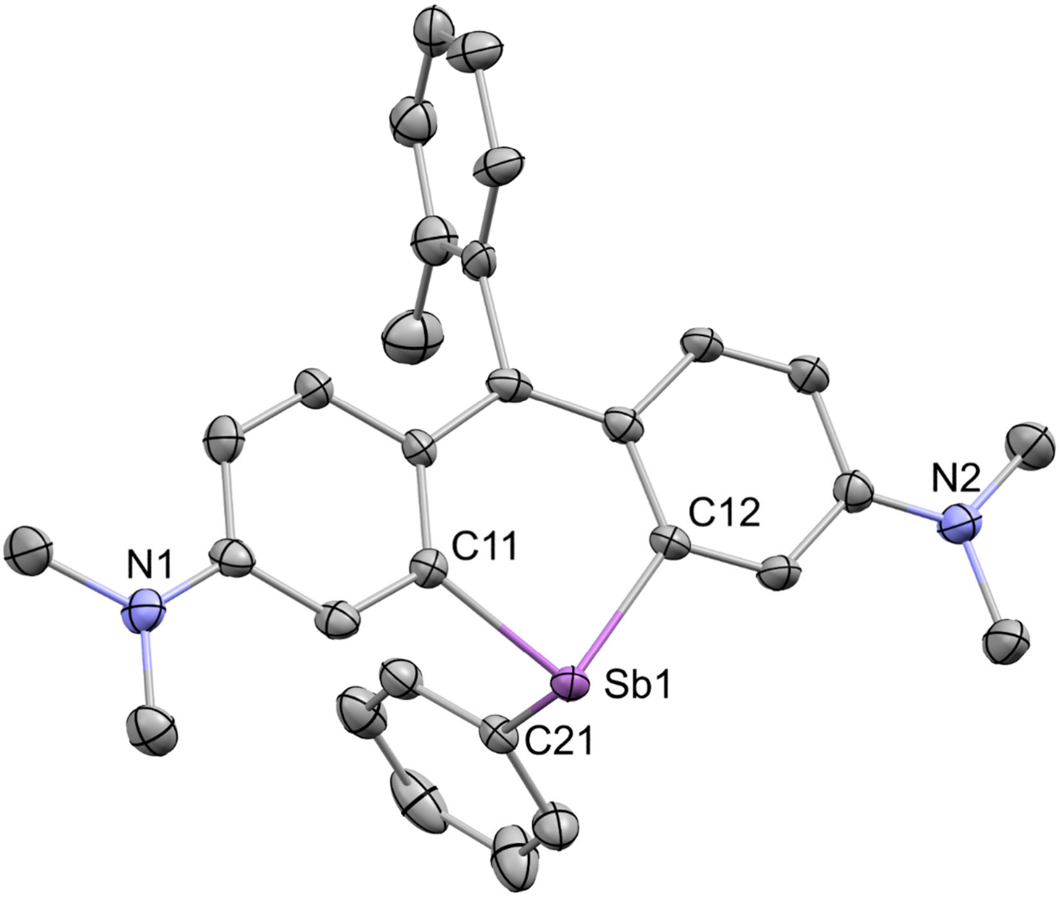

Figure 2: Crystal structure of one of the two independent molecules of [**6**]$^{+}$ in the crystals structure of [**2**][PF$_6$]. Ellipsoid are drawn at the 50% probability level. Hydrogen atoms are omitted for clarity. Selected bond lengths (Å) and angles (°) for the molecule shown (those for the second independent molecule are provided in brackets): Sb1-C11 2.130(6) [2.131(5)], Sb1C12 2.144(6) [2.133(6)], Sb1-C21 2.155(6) [2.167(6)], C11-Sb1-C12 92.2(2) [92.0(2)], C11-Sb1-C21 95.9(2) [94.8(2)], C12-Sb1-C21 91.9(2) [93.1(2)].

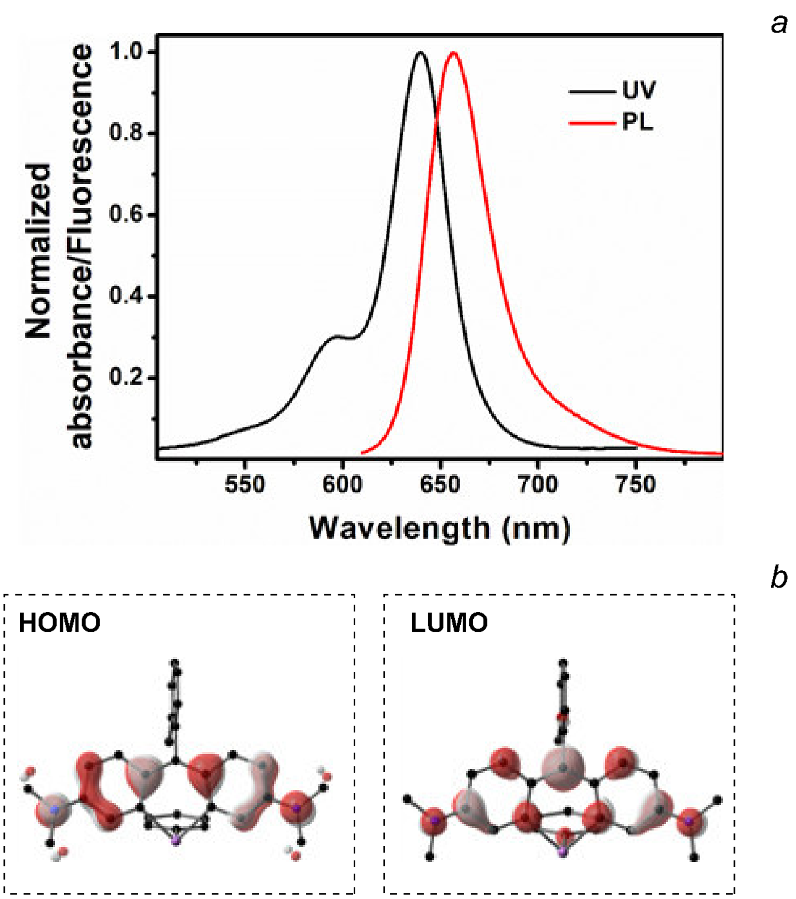

Figure 3: *a*) UV-Vis Absorption and fluorescence spectrum of [**6**]$^+$ in acetonitrile. *b*) HOMO (left) and LUMO (right) of [**6**]$^+$.

The UV-Vis absorption spectrum of [**6**]$^+$ displays a maximum absorbance at ~640 nm ($\varepsilon = 1.07\ 10^5\ M^{-1}cm^{-1}$) with a second, less intense, band at ~ 595 nm ($\varepsilon = 2.8\ 10^4\ M^{-1}cm^{-1}$) (Figure 3*a*). The fluorescence spectrum recorded with (excitation wavelength: 595 nm) shows an emission maximum at ~ 655 nm. These photophysical characteristics are reminiscent of those observed for related main group containing rhodamines such as the bismuth analog ([**4**]$^+$, Figure 1) which is also red light excitable, with an absorption maximum at 635 nm and an emission maximum at 658 nm when measured in buffered water at pH 7.4.[20] Given the possibility of heavy atom effect in this structure, we were eager to measure the fluorescence quantum yield of [**6**]$^+$. Measurements carried out using cresyl violet as a reference afforded a value 12%. This quantum yield is significantly higher than that of [**4**]$^+$ (3.9%) indicating that heavy atom effects play a less detrimental role in the case of [**6**]$^+$.[20] These effects cannot be entirely ruled out since the quantum yield of [**6**]$^+$ is lower than those measured for the silicon analogs.[15] Finally, the analogy between [**6**]$^+$ and its bismuth analog [**4**]$^+$ is also evident from an inspection of the frontier orbitals (Figure 3*b*) which were derived from DFT calculations carried out with the M062X functional and mixed basis set (Sb, cc-pVTZ-PP/ECP28; C/O/H, 6-31g; Cl, 6-311g(d)). Indeed, both the HOMO and LUMO of [**6**]$^+$ are almost analogous in shape and atomic parentage to those of [**4**]$^+$.

In summary, we have successfully synthesized and characterized the first antimony rhodamine. Our future efforts in the chemistry of this derivative will explore the oxidation of the antimony center and the use of the resulting derivatives for anion sensing.

Online Supplementary Materials

NMR, HRMS spectra, Spectroscopic Details. CCDC 2103824 contains the supplementary crystallographic data for this paper. These data can be obtained free of charge from The Cambridge Crystallographic Data Centre via www.ccdc.cam.ac.uk/data_request/cif.

Acknowledgment

This was work performed at Texas A&M University with support from the National Science Foundation (CHE-2108728), the Welch Foundation (A-1423), and Texas A&M University (Arthur E. Martell Chair of Chemistry). GRK thanks the Science and Engineering Research Board (SERB) of India for a postdoctoral Fellowship.

Footnotes

†*Crystal data for* 7. $C_{30}H_{30}N_2PF_6Sb$-0.576(CH_2Cl_2) (M = 734.21), triclinic, space group *P*-1 at 110 K: a = 10.598(2) Å, b = 14.737(3) Å and c = 21.110(4) Å, α = 72.95(3)°, β = 87.83(3)°, γ = 85.82 (3)°, V = 3143.3(12) Å^3, Z = 4, d_{calc} = 1.551 g cm^{-3}, μ(MoK$_\alpha$) = 1.086 mm^{-1}, F(000) = 1472.8. A total of 69976 reflections (R_{int} = 0.0852) were collected on a twinned (non-merohedral) crystal featuring two

components. The structure was refined using 16655 independent reflections of the major component [GOOF = 1.038; $wR_2 = 0.1552$ for all independent reflections; $R_1 = 0.0610$ for 11416 reflections with $I > 2\sigma(I)$]. The X-ray diffraction analysis was carried out on a Bruker APEX II CCD diffractometer (MoKα radiation, $\lambda = 0.71073$ Å, graphite monochromator). Semi-empirical absorption correction was performed using TWINABS program. [22] The structure was solved by direct methods (SHELXT)[23] and refined by least-squares procedures on F^2 using SHELXL[24] and OLEX2[25] was used to prepare material for publication. CCDC 2103824 contains the supplementary crystallographic data for this paper. These data can be obtained free of charge from The Cambridge Crystallographic Data Centre via http://www.ccdc.cam.ac.uk.

References

1 A. M. Christianson and F. P. Gabbaï, in *Main Group Strategies towards Functional Hybrid Materials* (Eds.: T. Baumgartner, F. Jaekle), John Wiley & Sons Ltd, Hoboken, NJ, 2018, pp. 405-432.
2 M. Hirai and F. P. Gabbaï, *Angew. Chem. Int. Ed.* 2015, **54**, 1205.
3 D. You, B. Zhou, M. Hirai and F. P. Gabbaï, *Org. Biomol. Chem.* 2021, **19**, 4949.
4 M. Hirai and F. P. Gabbaï, *Chem. Sci.* 2014, **5**, 1886.
5 I.-S. Ke, M. Myahkostupov, F. N. Castellano and F. P. Gabbaï, *J. Am. Chem. Soc.* 2012, **134**, 15309.
6 M. Hirai, M. Myahkostupov, F. N. Castellano and F. P. Gabbaï, *Organometallics* 2016, **35**, 1854.
7 A. M. Christianson and F. P. Gabbaï, *Chem. Commun.* 2017, **53**, 2471.
8 A. M. Christianson, E. Rivard and F. P. Gabbaï, *Organometallics* 2017, **36**, 2670.
9 A. M. Christianson and F. P. Gabbaï, *Organometallics* 2017, **36**, 3013.
10 J. Ohshita, R. Fujita, D. Tanaka, Y. Ooyama, N. Kobayashi, H. Higashimura and Y. Yamamoto, *Chem. Lett.* 2012, **41**, 1002.
11 J. Ohshita, K. Yamaji, Y. Ooyama, Y. Adachi, M. Nakamura and S. Watase, *Organometallics* 2019, **38**, 1516.
12 M. Li, Y. Li, X. Wang, X. Cui and T. Wang, *Chin. Chem. Lett.* 2019, **30**, 1682.
13 F. Deng and Z. Xu, *Chin. Chem. Lett.* 2019, **30**, 1667.
14 M. Grzybowski, M. Taki, K. Senda, Y. Sato, T. Ariyoshi, Y. Okada, R. Kawakami, T. Imamura and S. Yamaguchi, *Angew. Chem. Int. Ed.* 2018, **57**, 10137.
15 T. Ikeno, T. Nagano and K. Hanaoka, *Chem. Asian J.* 2017, **12**, 1435.
16 Y.-Q. Sun, J. Liu, X. Lv, Y. Liu, Y. Zhao and W. Guo, *Angew. Chem. Int. Ed.* 2012, **51**, 7634.
17 Y. Koide, Y. Urano, K. Hanaoka, T. Terai and T. Nagano, *ACS Chem. Biol.* 2011, **6**, 600.
18 Y. Koide, M. Kawaguchi, Y. Urano, K. Hanaoka, T. Komatsu, M. Abo, T. Terai and T. Nagano, *Chem. Commun.* 2012, **48**, 3091.
19 M. W. Kryman, G. A. Schamerhorn, J. E. Hill, B. D. Calitree, K. S. Davies, M. K. Linder, T. Y. Ohulchanskyy and M. R. Detty, *Organometallics* 2014, **33**, 2628.

20 T. Hirayama, A. Mukaimine, K. Nishigaki, H. Tsuboi, S. Hirosawa, K. Okuda, M. Ebihara and H. Nagasawa, *Dalton Trans.* 2017, **46**, 15991.
21 X. Zhou, R. Lai, J. R. Beck, H. Li and C. I. Stains, *Chem. Commun.* 2016, **52**, 12290.
22 G. M. Sheldrick, TWINABS, University of Göttingen, Germany
23 G. M. Sheldrick, SHELXTL, Version 6.1, Madison, Wisconsin, USA
24 G. M. Sheldrick, SHELXL-2014: Program for Crystal Structure Refinement, University of Göttingen, Germany
25 O. V. Dolomanov, L. J. Bourhis, R. J. Gildea, J. A. K. Howard and H. Puschmann, *J. Appl. Crystallogr.* 2009, **42**, 339.